Brief Papers

Nonlinear Attitude Observer Based on Range and Inertial Measurements

Sérgio Brás, *Student Member, IEEE*, Rita Cunha, Carlos Jorge Silvestre, *Member, IEEE*, and Paulo Jorge Oliveira, *Senior Member, IEEE*

***Abstract*— We address the problem of attitude and rate gyro bias estimation based on inertial and range data. Range measurements are obtained from beacons installed in an inertial frame and acoustic sensors fixed in the moving body reference frame. A nonlinear observer is proposed and its stability and performance properties are studied using Lyapunov techniques. In the presence of constant bias on the rate gyro measurements, the attitude and bias estimates are shown to converge exponentially to the desired values inside an almost global region of attraction. For time-varying bias with bounded derivative, a local result of ultimate boundedness is provided. The performance of the proposed nonlinear observer is validated experimentally using a high-accuracy calibration table, which provides ground-truth signals for comparison with the resulting estimates.**

***Index Terms*— Attitude estimation, Lyapunov method, nonlinear systems, observers.**

NOMENCLATURE

$\mathrm{O}(n)$	$:=\left\{\mathbf{U}\in\mathbb{R}^{n\times n} : \mathbf{U}\mathbf{U}^T=\mathbf{U}^T\mathbf{U}=\mathbf{I}\right\}$. Orthogonal Group of order n.
$\mathrm{SO}(n)$	$:=\left\{\mathcal{R}\in\mathbb{R}^{n\times n} : \det(\mathcal{R})=1\,\mathcal{R}^T\mathcal{R}=\mathbf{I}\right\}$. Special Orthogonal Group of order n.
$\mathrm{S}(n)$	$:=\left\{\mathbf{x}\in\mathbb{R}^{n+1} : \mathbf{x}^T\mathbf{x}=1\right\}$. n-dimensional sphere.
$\sigma_{\min}(\mathbf{A})$	Minimum singular value of matrix $\mathbf{A}$.
$\sigma_{\max}(\mathbf{A})$	Maximum singular value of matrix $\mathbf{A}$.
$[.]_\times$	Skew symmetric operator that maps $\mathbb{R}^3$ to the space of skew-symmetric matrices such that $[\mathbf{x}]_\times\mathbf{y}=\mathbf{x}\times\mathbf{y}$, $\mathbf{x},\mathbf{y}\in\mathbb{R}^3$.
$[.]_\otimes$	Unskew operator, that maps the space of skew-symmetric matrices to $\mathbb{R}^3$ such that $[[\mathbf{x}]_\times]_\otimes=\mathbf{x}$, $\mathbf{x}\in\mathbb{R}^3$.

Manuscript received December 4, 2011; accepted July 24, 2012. Manuscript received in final form August 14, 2012. Date of publication September 25, 2012; date of current version August 12, 2013. This work was supported in part by Fundação para a Ciência e a Tecnologia (FCT) under Project PEst-OE/EEI/LA0009/2011, Project PTDC/EEA-CRO/102857/2008 SCARVE, and Project PTDC/MAR/64546/2006 OBSERVFLY, and the EU Project TRIDENT of the EC-FP7. The work of S. Brás was supported by Fundação para a Ciência e a Tecnologia under Ph.D. Grant SFRH/BD/47456/2008. Recommended by Associate Editor A. Alessandri.

S. Brás, R. Cunha, and P. J. Oliveira are with the Laboratory of Robotics and Systems in Engineering and Science, Instituto Superior Técnico, Universidade Técnica de Lisboa, Lisbon 1049-001, Portugal (e-mail: sbras@isr.ist.utl.pt; rita@isr.ist.utl.pt; pjcro@isr.ist.utl.pt).

C. J. Silvestre is with the Laboratory of Robotics and Systems in Engineering and Science, Instituto Superior Técnico, Universidade Técnica de Lisboa, Lisbon 1049-001, Portugal, and also with the Department of Electrical and Computer Engineering, Faculty of Science and Technology, University of Macau, Taipa, China (e-mail: cjs@isr.ist.utl.pt).

Color versions of one or more of the figures in this paper are available online at http://ieeexplore.ieee.org.

Digital Object Identifier 10.1109/TCST.2012.2213821

I. INTRODUCTION

ATTITUDE estimation plays an important role in many modern platforms, such as aircrafts, satellites, unmanned air vehicles, and underwater autonomous robots. It is a classical estimation problem that, despite its rich historical background, continues to attract intensive research efforts and to experiencing new advances. Over the years, a wide variety of estimation techniques have been proposed to address this problem. Some solutions are purely algebraic, like the solution to Wahba's problem [1]. More advanced solutions rely on the system dynamics to obtain better accuracy and noise reduction, as is the case with Kalman filtering-based approaches [2]. Among the latter, the extended Kalman filter (EKF), has been widely used to address nonlinear estimation problems [3]–[5]. Recently, other solutions have been proposed to overcome the limitations of the EKF in estimating states evolving on the group of rotations SO(3), namely, the multiplicative extended Kalman filter (MEKF) [6] and the invariant extended Kalman filter [7]. However, none of the EKF-based estimators guarantees optimality or convergence. Among the dynamic estimators, nonlinear observers have emerged as an attractive alternative given the possibility to establish convergence bounds and provide stability guarantees. In many applications, it is desirable to design observers based only on the rigid body kinematics, which are an exact description of the physical quantities involved, see [8] and [9]. Attitude observers rigorously formulated on non-Euclidean spaces, such as the set of rotation matrices SO(3) and the set of unit quaternions S(3), can be found in [10]–[14]. Guidelines on observer design and the topological limitation for achieving global stabilization on the SO(3) manifold are discussed in [15]–[17]. In the design of attitude observers, it is often assumed that the bias in the angular velocity measurements is constant [11], [13], [14]. In [18], the authors take a different approach and estimate a time-varying rate gyro bias assuming that its time evolution is determined by a known linear model with known inputs. However, in many situations, such a model is not available or it depends on unknown inputs. In our approach, we assume constant bias in the design of the observer and study the stability properties of the observer when this assumption does not hold.

The EKF-type estimators and the nonlinear observers combine the information from different sources. The non-ideal characteristics of the inertial sensors, namely bias, misalignment, and noise, render inaccurate the attitude obtained by the integration of inertial data. External aiding sensors, such as global positioning system (GPS) receivers, must be included to obtain more accurate estimates. However, in

GPS-denied environments, such as indoors or in the vicinity of buildings and other structures, alternative aiding sensors are required. For that reason, many proposed solutions in the field of robotics rely on range data. Range measurements can be obtained using sensors such as laser range finders and stereo cameras. An affordable alternative is the use of acoustic sensors. In the Cricket system [19], an acoustic signal and a radio frequency (RF) synchronization signal are transmitted simultaneously. The receiver then measures the time difference between both signals and computes the distance using the speed of sound in the air. Other advantages of these sensors are their compact size and low power consumption.

This brief presents a nonlinear attitude observer that combines angular rate measurements acquired by nonideal rate gyros with range measurements provided by a commercially available acoustic positioning system, which comprises an ultrasonic beacon array assumed fixed in the inertial frame and an acoustic receiver array installed on board the vehicle. The proposed solution builds on previous work [20]–[22] to consider the specific problem of attitude estimation based on angular rate measurements and position measurements that are extracted from the range data. It is shown that, in the presence of constant bias on the rate gyros, the attitude and bias estimation errors converge exponentially fast to the origin in any closed neighborhood of the almost global region of attraction. When compared with other attitude observers proposed in the literature, (see [8], [9], [11]–[14], and references therein), this brief presents new results on the stability analysis of the system. More specifically, using a Lyapunov coordinate transformation, we show that worst case bounds on the convergence rates can be explicitly computed. Assuming that the bias on the rate gyros is time-varying, the estimation errors are shown to remain bounded for sufficiently small initial conditions with ultimate bounds proportional to the bias time derivatives. Moreover, based on the Kalman–Bucy filter theory, a method is proposed for selecting observer gains such that the covariance of the estimation error in the vicinity of the origin is minimized. Detailed experiments are conducted with a custom-built prototype that comprises a Memsense nIMU and a Cricket localization system [19]. For real-time evaluation of the proposed solution, the experimental setup was assembled and mounted on an Ideal Aerosmith positioning rate table system, Model 2103HT [23], which is a three-axis system that provides precise angular position, rate, and acceleration measurements. A comparison between the experimental results obtained with the filter and those given by the MEKF technique illustrates the advantages of the proposed solution.

To summarize, the main contributions of this brief are the following.

1) A range-based nonlinear attitude observer is presented that relies on geometric methods to guarantee almost global asymptotic stability of the desired equilibrium point.
2) An alternative description for the estimation error dynamics is obtained by applying a time-varying Lyapunov transformation. This novel description takes the form of an linear time-varying system and significantly simplifies the stability analysis and enables other novelties of this brief.
3) Computation of explicit bounds on the estimation error is carried out in the presence of time-varying rate gyro bias based on the new description of the error.
4) An explicit method to tune the observer gains is presented such that the covariance of the estimation error in the vicinity of the desired equilibrium point is minimized.
5) Experimental results attest the feasibility of the proposed solution, and a comparison with the MEKF is made.

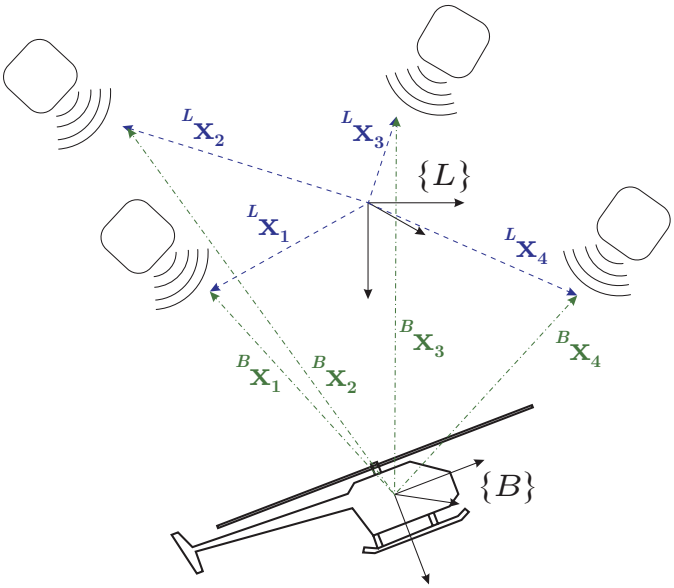

Fig. 1. Frames and navigation system configuration.

The rest of this brief is structured as follows. In Section II, the attitude estimation problem is introduced and the sensor suite is described. In Section III, the nonlinear attitude observer is presented and its properties are highlighted. A method to tune the observer gains based on the Kalman–Bucy filter is proposed in Section IV. The experimental setup is described in Section V. In Section VI, experimental results validating the performance of the proposed solution are presented. Finally, concluding remarks are given in Section VII.

II. Problem Formulation

In this section, the attitude estimation problem is introduced and the sensor suite is characterized. Consider the two reference frames depicted in Fig. 1, the local reference frame $\{L\}$, which is placed in the mission scenario, and the reference frame $\{B\}$ attached to the rigid body. For the sake of simplicity, $\{L\}$ is assumed to be an inertial frame.

Let $\mathcal{R} \in \mathrm{SO}(3)$ be the rotation matrix that transforms the vectors expressed in $\{B\}$ to $\{L\}$ and $\boldsymbol{\omega} \in \mathbb{R}^3$ the rigid body angular velocity expressed in $\{B\}$. The rigid body attitude kinematics is described by the differential equation

$$\dot{\mathcal{R}} = \mathcal{R}[\boldsymbol{\omega}]_\times.$$

The sensor suite comprises a triad of rate gyros and an acoustic positioning system. The angular velocity measurements $\boldsymbol{\omega}_r \in \mathbb{R}^3$ are assumed to be corrupted by a constant unknown bias term $\mathbf{b} \in \mathbb{R}^3$ so that

$$\boldsymbol{\omega}_r = \boldsymbol{\omega} + \mathbf{b}.$$

The basic elements of the acoustic positioning system are an array of beacons placed in the mission scenario and an array of receivers installed on the vehicle. The range from each beacon to all acoustic receivers can then be measured. Let the position of the ith beacon in $\{L\}$ and in $\{B\}$ be denoted by ${}^L\mathbf{x}_i \in \mathbb{R}^3$ and by ${}^B\mathbf{x}_i \in \mathbb{R}^3$, respectively, where $i = 1, \ldots, N_b$, and N_b is the number of beacons. We resort to the spherical interpolation method proposed in [24] to obtain the positions of the beacons in $\{B\}$; so ${}^B\mathbf{x}_i$ and ${}^L\mathbf{x}_i$, $i = 1, \ldots, N_b$ are available in the filter. The spherical interpolation method requires the existence of at least four noncoplanar receivers, i.e., $N_b \geq 4$.

Let ${}^B\mathbf{X} = [{}^B\mathbf{x}_1 \ \cdots \ {}^B\mathbf{x}_{N_b}] \in \mathbb{R}^{3\times N_b}$ and ${}^L\mathbf{X} = \mathcal{R}\,{}^B\mathbf{X} = [{}^L\mathbf{x}_1 \ \cdots \ {}^L\mathbf{x}_{N_b}] \in \mathbb{R}^{3\times N_b}$. Without loss of generality, the origin of the local frame $\{L\}$ is defined at the centroid of the beacons. Therefore, the vectors ${}^L\mathbf{x}_i$, $i = 1, \ldots, N_b$, satisfy $\sum_{i=1}^{N_b} {}^L\mathbf{x}_i = 0$.

The observer uses measurements in the form ${}^B\mathbf{u}_i$, $i = 1, \ldots, N_b$, which are obtained using a conveniently defined coordinate transformation. This transformation takes the form

$${}^B\mathbf{U} = {}^B\mathbf{X}\mathbf{D}_X\mathbf{A}_X$$

where ${}^B\mathbf{U} \in \mathbb{R}^{3\times N_b-1}$, $\mathbf{D}_X = \begin{bmatrix} \mathbf{0}_{1\times N_b-1} \\ \mathbf{I}_{N_b-1} \end{bmatrix} - \begin{bmatrix} \mathbf{I}_{N_b-1} \\ \mathbf{0}_{1\times N_b-1} \end{bmatrix}$ and $\mathbf{A}_X \in \mathbb{R}^{N_b-1\times N_b-1}$. The representation of the position measurements in the local reference frame $\{L\}$ is given by ${}^L\mathbf{U} = \mathcal{R}\,{}^B\mathbf{U} = {}^L\mathbf{X}\mathbf{D}_X\mathbf{A}_X$. Since the beacons are placed in known locations of the mission scenario, the matrix ${}^L\mathbf{U}$ is known *a priori*.

The measurements directionality is made uniform by the nonsingular linear transformation $\mathbf{A}_X$, i.e., ${}^B\mathbf{U}\,{}^B\mathbf{U}^T = \mathbf{I}$. Such linear transformation can be obtained resorting to the singular value decomposition of ${}^L\mathbf{X}\mathbf{D}_X = \mathbf{W}\mathbf{S}\mathbf{V}^T$, where $\mathbf{W} \in \mathrm{O}(3)$, $\mathbf{V} \in \mathrm{O}(N_b-1)$, $\mathbf{S} = [\mathrm{diag}(s_1, s_2, s_3)\ \mathbf{0}_{3\times(N_b-4)}]$. The following assumption is necessary to compute the transformation $\mathbf{A}_X$.

Assumption 1: The positions of the beacons are not collinear, i.e., $\mathrm{rank}({}^L\mathbf{X}) \geq 2$.

If ${}^L\mathbf{X}\mathbf{D}_X$ is full rank, let

$$\mathbf{A}_X = \mathbf{V}\begin{bmatrix} \mathrm{diag}(s_1, s_2, s_3)^{-1} & \mathbf{0}_{3\times(N_b-4)} \\ \mathbf{0}_{(N_b-4)\times 3} & \mathbf{I}_{(N_b-4)\times(N_b-4)} \end{bmatrix}.$$

Then, due to the orthogonality of $\mathbf{W}$ and $\mathbf{V}$, it follows that ${}^L\mathbf{U}\,{}^L\mathbf{U}^T = {}^L\mathbf{X}\mathbf{D}_X\mathbf{A}_X({}^L\mathbf{X}\mathbf{D}_X\mathbf{A}_X)^T = \mathbf{I}$, and since ${}^L\mathbf{U} = \mathcal{R}\,{}^B\mathbf{U}$, we have that ${}^B\mathbf{U}\,{}^B\mathbf{U}^T = \mathbf{I}$. If $[{}^L\mathbf{x}_1 \ \cdots \ {}^L\mathbf{x}_{N_b}]$ is of rank 2, ${}^L\mathbf{X}$ needs to be redefined as ${}^L\mathbf{X} = [{}^L\mathbf{x}_1 \ \cdots \ {}^L\mathbf{x}_{N_b}, {}^L\mathbf{x}_i \times {}^L\mathbf{x}_j]$, for some i and j such that ${}^L\mathbf{x}_i \times {}^L\mathbf{x}_j \neq \mathbf{0}$, in order to obtain a full-rank matrix.

Note that the matrix $\mathbf{A}_X$ is constant along the system trajectories since it is computed using the position of the beacons in $\{L\}$ which are fixed. It is convenient to orthogonalize the measured directions in order to simplify the derivation of the observer feedback law.

In this brief, we rely on range measurements to obtain the positions ${}^B\mathbf{x}_1, \ldots, {}^B\mathbf{x}_{N_b}$. Other alternatives are available that provide such measurements. Nevertheless, from the application point of view, the use of ultrasonic beacons is still very relevant, since range measurements are widely used in many robotic applications in great part due to their flexibility and the availability of compact and low-power sensors. With proper modifications to the proposed algorithm, other sensors, such as magnetometers and gravimeters, can also be used. These sensors have, however, their own limitations.

The objective of this brief is to exploit the information provided by the sensor suite by deriving an attitude observer that combines the inertial measurements with ranges between a beacon array and a receiver array.

III. Attitude Observer

In this section, the attitude observer, which relies on the sensors' measurements to estimate simultaneously the rigid body attitude and rate gyro bias, is presented and its properties are derived. It is shown that the proposed feedback law yields exponential convergence of the estimation error for almost all initial conditions, in the sense that only a set of measure zero lies outside the region of attraction.

The proposed observer takes the form

$$\dot{\hat{\mathcal{R}}} = \hat{\mathcal{R}}[\hat{\boldsymbol{\omega}}]_\times \tag{1a}$$

$$\hat{\boldsymbol{\omega}} = {}^B\hat{\mathbf{U}}\,{}^B\mathbf{U}^T(\boldsymbol{\omega}_r - \hat{\mathbf{b}}) - k_\omega \mathbf{s}_\omega \tag{1b}$$

$$\dot{\hat{\mathbf{b}}} = k_b \mathbf{s}_\omega \tag{1c}$$

$$\mathbf{s}_\omega = [{}^B\mathbf{U}\,{}^B\hat{\mathbf{U}}^T - {}^B\hat{\mathbf{U}}\,{}^B\mathbf{U}^T]_\otimes \tag{1d}$$

where $\hat{\mathcal{R}} \in \mathrm{SO}(3)$ is the estimated attitude, $\hat{\mathbf{b}} \in \mathbb{R}^3$ is the estimated rate gyro bias, $k_\omega, k_b \in \mathbb{R}$ are positive gains, the term ${}^B\hat{\mathbf{U}} = \hat{\mathcal{R}}^T\,{}^L\mathbf{U}$ is a function of the observer estimates and known quantities, and the term ${}^B\mathbf{U} = {}^B\mathbf{X}\mathbf{D}_X\mathbf{A}_X$ is an explicit function of the sensor measurements.

Let the attitude and bias estimation errors be given by $\tilde{\mathcal{R}} = \hat{\mathcal{R}}^T\mathcal{R}$ and $\tilde{\mathbf{b}} = \hat{\mathbf{b}} - \mathbf{b}$, respectively, and note that, since ${}^L\mathbf{U}\,{}^L\mathbf{U}^T = \mathbf{I}$ and ${}^B\mathbf{U} = \mathcal{R}^T\,{}^L\mathbf{U}$, the term $\mathbf{s}_\omega$ satisfies $\mathbf{s}_\omega = [\tilde{\mathcal{R}}^T - \tilde{\mathcal{R}}]_\otimes$. The error dynamics are autonomous and given by

$$\begin{aligned} \dot{\tilde{\mathcal{R}}} &= k_\omega \tilde{\mathcal{R}}(\tilde{\mathcal{R}}^T - \tilde{\mathcal{R}}) + \tilde{\mathcal{R}}[\tilde{\mathbf{b}}]_\times \\ \dot{\tilde{\mathbf{b}}} &= k_b[\tilde{\mathcal{R}}^T - \tilde{\mathcal{R}}]_\otimes. \end{aligned} \tag{2}$$

Let the Euler angle-axis parameterization of $\tilde{\mathcal{R}}$ be described by the rotation vector $\boldsymbol{\lambda} \in \mathbb{R}^3$ and by the rotation angle $\theta \in [0\ \pi]$, such that $\tilde{\mathcal{R}} = \mathrm{rot}(\theta, \boldsymbol{\lambda}) = \cos(\theta) + \sin(\theta)[\boldsymbol{\lambda}]_\times + (1-\cos(\theta))\boldsymbol{\lambda}\boldsymbol{\lambda}^T$ [25]. The following lemma provides sufficient conditions on the initial estimates for the boundedness of the estimation errors, which excludes the set of points such that $\tilde{\mathcal{R}} = \mathrm{rot}(\pi, \boldsymbol{\lambda})$, $\boldsymbol{\lambda} \in \mathbb{R}^3$.

Lemma 1: For any initial condition satisfying

$$\frac{||\tilde{\mathbf{b}}(t_0)||^2}{2(1+\cos(\theta(t_0)))} < k_b \tag{3}$$

the estimation errors $\tilde{\mathbf{x}} = (\tilde{\mathcal{R}}, \tilde{\mathbf{b}})$ are bounded, and there exists $\omega_{\max} \in \mathbb{R}^3$ such that the attitude error satisfies $0 \leq \theta(t) \leq \theta_{\max} < \pi$ for all $t \geq t_0$.

Proof: Consider the following Lyapunov function:

$$V = \frac{||\tilde{\mathcal{R}} - \mathbf{I}||^2}{2} + \frac{1}{2k_b}||\tilde{\mathbf{b}}||^2 = 2(1 - \cos(\theta)) + \frac{1}{2k_b}||\tilde{\mathbf{b}}||^2 \quad (4)$$

where $\|.\|$ denotes the Frobenius norm of matrices and the Euclidean norm of vectors. The time derivative of V is given by

$$\begin{aligned}\dot{V} &= -\operatorname{tr}(\dot{\tilde{\mathcal{R}}}) + \frac{1}{k_b}\tilde{\mathbf{b}}^T\dot{\tilde{\mathbf{b}}} \\ &= -\operatorname{tr}(\tilde{\mathcal{R}}[-\tilde{\mathcal{R}}^T\hat{\boldsymbol{\omega}} + \boldsymbol{\omega}]_\times) + \frac{1}{k_b}\tilde{\mathbf{b}}^T\dot{\tilde{\mathbf{b}}} \\ &= \mathbf{s}_\omega^T(\tilde{\mathcal{R}}^T\hat{\boldsymbol{\omega}} - \boldsymbol{\omega}) + \frac{1}{k_b}\tilde{\mathbf{b}}^T\dot{\tilde{\mathbf{b}}}.\end{aligned}$$

Since (1b) can be rewritten in the form $\hat{\boldsymbol{\omega}} = \tilde{\mathcal{R}}(\boldsymbol{\omega} - \tilde{\mathbf{b}}) - k_\omega \mathbf{s}_\omega$, along the trajectories of the closed-loop system (2), $\dot{V}$ takes the form $\dot{V} = -k_\omega\|\mathbf{s}_\omega\|^2$.

Let $\boldsymbol{\Omega}_\rho = \{\tilde{\mathbf{x}} \in D_b : V \leq \rho\}$, where $\rho \in \mathbb{R}^+$. As the Lyapunov function (4) is a weighted squared distance from the desired equilibrium point, the set $\boldsymbol{\Omega}_\rho$ is a compact set. The derivative of the Lyapunov function satisfies $\dot{V} \leq 0$, which means that any trajectory starting in $\boldsymbol{\Omega}_\rho$ remains in $\boldsymbol{\Omega}_\rho$. Then, for all $t \geq t_0$ the state is bounded.

The gain condition (3) is equivalent to $V(\tilde{\mathbf{x}}(t_0)) < 4$. The invariance of $\boldsymbol{\Omega}_\rho$ implies that $V(\tilde{\mathbf{x}}(t)) \leq V(\tilde{\mathbf{x}}(t_0))$, then $2(1 - \cos(\theta(t))) \leq 2(1 - \cos(\theta_{\max})) = V(\tilde{\mathbf{x}}(t_0)) < 4$ and consequently $\theta(t) \leq \theta_{\max} < \pi$ for all $t \geq t_0$. ∎

In general, one does not know the values of $\tilde{\mathbf{b}}(t_0)$ and $\cos(\theta(t_0))$ required in (3). However, in practice, one can use the information provided by the manufacturer of the sensors to obtain worst case values for both quantities.

The proposed observer is derived on SO(3) in order to overcome the problems associated with unwinding phenomena and singularities introduced by other attitude representations. However, to gain further insight into the properties of the error system (2), it is convenient to rewrite it using the attitude vector $\tilde{\mathbf{q}}_v = \sin(\theta/2)\boldsymbol{\lambda}$ and apply an adequately defined Lyapunov transformation to obtain a more tractable system. We can analyze the properties of the error of the observer using this representation since $\|\tilde{\mathcal{R}} - \mathbf{I}\|^2 = 8\|\tilde{\mathbf{q}}_v\|^2$. Using $\tilde{\mathbf{q}}_v$ instead of $\tilde{\mathcal{R}}$ in the state vector yields

$$\begin{aligned}\dot{\tilde{\mathbf{q}}}_v &= -2k_\omega\tilde{q}_s^2\tilde{\mathbf{q}}_v + \frac{1}{2}(\tilde{q}_s\mathbf{I} + [\tilde{\mathbf{q}}_v]_\times)\tilde{\mathbf{b}} \\ \dot{\tilde{\mathbf{b}}} &= -4k_b\tilde{q}_s\tilde{\mathbf{q}}_v \end{aligned} \quad (5)$$

where $\tilde{q}_s = \cos(\theta/2)$. Consider the following coordinate transformation: $\boldsymbol{\eta}_1 = 2\mathbf{T}(t)\tilde{\mathbf{q}}_v$, $\boldsymbol{\eta}_2 = 1/\sqrt{2k_b}\mathbf{T}(t)\tilde{\mathbf{b}}$, where $\mathbf{T}(t) \in \mathrm{SO}(3)$ is a rotation matrix that integrates the rate gyro bias

$$\dot{\mathbf{T}}(t) = \frac{1}{2}\mathbf{T}(t)[\tilde{\mathbf{b}}]_\times. \quad (6)$$

The time derivative of the transformed state vector $\boldsymbol{\eta} = [\boldsymbol{\eta}_1^T\boldsymbol{\eta}_2^T]^T$ is given by

$$\dot{\boldsymbol{\eta}} = \mathbf{A}(\boldsymbol{\eta})\boldsymbol{\eta} \quad (7)$$

where

$$\mathbf{A}(\boldsymbol{\eta}) = \begin{bmatrix} -2k_\omega\tilde{q}_s^2\mathbf{I} & \sqrt{2k_b}\tilde{q}_s\mathbf{I} \\ -\sqrt{2k_b}\tilde{q}_s\mathbf{I} & \mathbf{0} \end{bmatrix}.$$

Since $\mathbf{T}(t)$ is a rotation matrix, it satisfies $||\mathbf{T}(t)|| = \det(\mathbf{T}(t)) = 1$ for all $t \geq t_0$. Hence, $\mathbf{T}(t)$ is a Lyapunov transformation [26] and the stability properties of (7) also hold for (5).

The following theorem characterizes the stability of the error dynamics (7) and consequently (2), showing that the origin is exponentially stable given bounded initial estimation errors.

Theorem 1: For any initial condition that satisfies (3)

$$\frac{||\tilde{\mathbf{b}}(t_0)||^2}{2(1 + \cos(\theta(t_0)))} < k_b$$

the error dynamics converge exponentially to the stable equilibrium point $(\tilde{\mathcal{R}}, \tilde{\mathbf{b}}) = (\mathbf{I}, \mathbf{0})$.

Proof: In order to prove the exponential convergence of (7), it is sufficient to show that there exists positive constants a, k_1, k_2, k_3 and a continuously differentiable function V_T such that [27, Th. 4.10]

$$\begin{aligned} k_1\|\boldsymbol{\eta}\|^a \leq V_T(t, \boldsymbol{\eta}) \leq k_2\|\boldsymbol{\eta}\|^a \\ \frac{\partial V_T}{\partial t} + \frac{\partial V_T}{\partial \boldsymbol{\eta}}\mathbf{A}(\boldsymbol{\eta})\boldsymbol{\eta} \leq -k_3\|\boldsymbol{\eta}\|^a. \end{aligned}$$

In particular, these conditions are satisfied if the function V_T takes the form

$$V_T(\boldsymbol{\eta}) = \boldsymbol{\eta}^T\mathbf{P}\boldsymbol{\eta} > 0 \quad (8)$$

$$\dot{V}_T(\boldsymbol{\eta}, t) = -\boldsymbol{\eta}^T\mathbf{Q}(\boldsymbol{\eta})\boldsymbol{\eta} < 0 \quad (9)$$

where $\mathbf{P} \in \mathbb{R}^{6\times6}$ and $\mathbf{Q}(\boldsymbol{\eta}) \in \mathbb{R}^{6\times6}$ are symmetric positive definite matrices and the minimum singular value of $\mathbf{Q}(\boldsymbol{\eta})$, denoted by $\sigma_{\min}(\mathbf{Q}(\boldsymbol{\eta}))$, is uniformly lower bounded by a nonzero positive constant. In what follows, the dependency of $\mathbf{A}$ and $\mathbf{Q}$ on $\boldsymbol{\eta}$ is omitted for reasons of simplicity. Let

$$\mathbf{P} = \begin{bmatrix} p_{11}\mathbf{I}_{3\times3} & p_{12}\mathbf{I}_{3\times3} \\ p_{12}\mathbf{I}_{3\times3} & p_{22}\mathbf{I}_{3\times3} \end{bmatrix}$$

$$\mathbf{Q} = \begin{bmatrix} q_{11}\mathbf{I}_{3\times3} & q_{12}\mathbf{I}_{3\times3} \\ q_{12}\mathbf{I}_{3\times3} & q_{22}\mathbf{I}_{3\times3} \end{bmatrix}$$

where $p_{11}, p_{12}, p_{22}, q_{11}, q_{12}, q_{22} \in \mathbb{R}$ and $\mathbf{Q} = -(\mathbf{PA} + \mathbf{A}^T\mathbf{P})$. In order to satisfy (8) and (9), it is sufficient to show that the leading principal minors of $\mathbf{P}$ and $\mathbf{Q}$ are strictly positive

$$p_{11} > 0 \quad (10)$$

$$p_{11}p_{22} - p_{12}^2 > 0 \quad (11)$$

$$q_{11} > 0 \quad (12)$$

$$q_{11}q_{22} - q_{12}^2 > 0. \quad (13)$$

Using some algebraic manipulations on the inequalities (10)–(13), we derive sufficient conditions for p_{11}, p_{12}, and p_{22} so that (8) and (9) hold. The condition (13) can be expanded in the form

$$\left(4k_\omega\tilde{q}_s^2p_{11} + 2\sqrt{2k_b}\tilde{q}_sp_{12}\right)\left(-2\sqrt{2k_b}\tilde{q}_sp_{12}\right) - \left(2k_\omega\tilde{q}_s^2p_{12} - \sqrt{2k_b}\tilde{q}_sp_{11} + \sqrt{2k_b}\tilde{q}_sp_{22}\right)^2 > 0. \quad (14)$$

Using $\tilde{q}_s = \cos(\theta/2)$ and assuming that Lemma 1 holds, it is easy to show that $\tilde{q}_{s\min} \leq \tilde{q} \leq 1$, where $\tilde{q}_{s\min} = \cos(\theta_{\max}/2) > 0$. Consequently, $\tilde{q}_s$ can be factored out of (14). Let $p_{11} = p_{22}$; then if

$$-\frac{2k_\omega \tilde{q}_s}{\sqrt{2k_b} + \frac{k_\omega^2 \tilde{q}_s^2}{\sqrt{2k_b}}} p_{11} < p_{12} < 0 \tag{15}$$

the inequality (14) is satisfied. Equation (12) is equivalent to

$$-\frac{2k_\omega \tilde{q}_s}{\sqrt{2k_b}} p_{11} < p_{12} < 0. \tag{16}$$

Note that any p_{12} that satisfies (15) also satisfies (16). Since $\tilde{q}_s \geq \tilde{q}_{s_{\min}} > 0$, we can conclude that, for any positive $p_{11} = p_{22}$, there exists a p_{12} such that (11)–(13) are satisfied. Also note that for any choice of p_{12} satisfying (13), $|\det(\mathbf{Q})|$ does not converge to zero along time and all elements of $\mathbf{Q}$ are finite. Together, these two properties guarantee that $\sigma_{\min}(\mathbf{Q})$ is lower bounded by a positive constant, and hence the conditions that guarantee exponential convergence of the errors to zero are satisfied. ■

This proof exploits a new Lyapunov transformation given by (6) and resorts to the positive definite matrices $\mathbf{P}$ and $\mathbf{Q}$ to show that the errors converge exponentially to the desired equilibrium point. Using the constraints for positive definiteness, $\mathbf{P}$ and $\mathbf{Q}$ can be explicitly computed to provide exponential convergence bounds and worst case convergence rates as specified in

$$||\boldsymbol{\eta}(t)|| \leq \left(\frac{\sigma_{\max}(\mathbf{P})}{\sigma_{\min}(\mathbf{P})}\right)^{\frac{1}{2}} ||\boldsymbol{\eta}(t_0)|| e^{-\frac{\sigma_{\min}(\mathbf{Q})}{2\sigma_{\max}(\mathbf{P}))}(t-t_0)}.$$

Note that, for purposes of analysis, different values for the parameter p_{12} can be selected so as to reach different conclusions about the system. If p_{12} is close to zero, the value of $\sigma_{\max}(\mathbf{P})/\sigma_{\min}(\mathbf{P})$ is close to 1, so we obtain a larger basin of attraction. Choosing a smaller value for p_{12}, we obtain a higher $\sigma_{\min}(\mathbf{Q})$ and consequently a higher value for the lower bound on the convergence rate.

Corollary 1: Assume that the initial estimation errors are bounded according to

$$\theta(t_0) \leq \theta_{\max} \qquad ||\tilde{\mathbf{b}}|| \leq b_{0_{\max}} \tag{17}$$

where $(1 - \cos(\theta_{\max})) < 2$, and select k_{b_ω} such that

$$\frac{b_{0_{\max}}}{4(1 + \cos(\theta(t_0)))} < k_{b_\omega}.$$

Then, the origin $(\tilde{\mathcal{R}}, \tilde{\mathbf{b}}) = (\mathbf{I}, \mathbf{0})$ is uniformly exponentially stable in the set defined by (17).

In Theorem 1 and Corollary 1, we have assumed that the rate gyro bias is constant. In practice, the bias suffers fluctuations that depend on several parameters, such as temperature, power supply, or g-sensitivities. If the constant bias assumption is lifted, the convergence result of Theorem 1 no longer holds. However, we can show that for bias values with bounded time derivative $||\dot{\mathbf{b}}|| < \gamma$, the estimation errors are also bounded with ultimate bound proportional to γ.

Lemma 2: Consider the attitude observer defined in (1) and assume that $\dot{\mathbf{b}}$ is bounded, with $||\dot{\mathbf{b}}|| < \gamma$. Then, for a sufficiently small γ, there is a sufficiently small error on the initial estimates such that the estimation errors are bounded with ultimate bound proportional to γ.

Proof: Define the domain $U = \{\boldsymbol{\eta} : V_T(\boldsymbol{\eta}) \leq 4 - \epsilon\}$, $0 < \epsilon < 4$. From Theorem 1 we know that, if k_b satisfies (3), there exist positive constants k_1, k_2, k_3, and k_4 such that

$$\begin{aligned} k_1||\boldsymbol{\eta}||^2 &\leq V_T(t, \boldsymbol{\eta}) \leq k_2||\boldsymbol{\eta}||^2 \\ \dot{V}_T(t, \boldsymbol{\eta}) &\leq -k_3||\boldsymbol{\eta}||^2 \\ \left\| \frac{\partial V_T}{\partial \boldsymbol{\eta}} \right\| &\leq k_4||\boldsymbol{\eta}||. \end{aligned}$$

In particular, we can choose $k_1 = \sigma_{\min}(\mathbf{P})$, $k_2 = \sigma_{\max}(\mathbf{P})$, $k_3 = \sigma_{\min}(\mathbf{Q})$, and $k_4 = 2\sigma_{\max}(\mathbf{P})$. It follows that, if $\dot{\mathbf{b}} \neq 0$, the time derivative of V_T is given by

$$\dot{V}_T \leq -k_3||\boldsymbol{\eta}||^2 + k_4\kappa\|\boldsymbol{\eta}\|\|\dot{\mathbf{b}}\|$$

where $\kappa = 1/\sqrt{2k_b}$. Assuming $\|\dot{\mathbf{b}}\| \leq \gamma$ implies that $\dot{V}_T < 0$ for $\|\boldsymbol{\eta}\| > k_4/k_3\kappa\gamma$ and $\|\boldsymbol{\eta}\| < \sqrt{4-\epsilon}$. To ensure that $\|\boldsymbol{\eta}(t)\|$ does not exceed the upper bound $\sqrt{4-\epsilon}$, the initial conditions must satisfy $\|\boldsymbol{\eta}(t_0)\| < \sqrt{k_1/k_2(4-\epsilon)}$. Then, if γ is sufficiently small, we can guarantee that $k_4/k_3\kappa\gamma < \sqrt{k_1/k_2(4-\epsilon)} < \sqrt{4-\epsilon}$, and $\boldsymbol{\eta}(t)$ remains in U for all $t \geq t_0$. Since $\dot{V}_T < 0$ for $k_4/k_3\kappa\gamma < \|\boldsymbol{\eta}\| < \sqrt{4-\epsilon}$, we can conclude that $\|\boldsymbol{\eta}\|$ is ultimately bounded by $\sqrt{k_2/k_1}k_4/k_3\kappa\gamma$. ■

IV. Tuning the Observer

The technique adopted to obtain the attitude observer is naturally suited for tackling uncertainties such as the presence of a constant bias in the rate gyros, but renders the handling of others, such as random noise, not straightforward. However, it is possible to exploit the observer structure and consider the characteristics of the sensor noise to tune the feedback gains k_ω and k_b.

In (1b) and (1c), the terms ${}^B\mathbf{U}$, $\boldsymbol{\omega}_r$ and $\mathbf{s}_\omega$ depend on the sensor measurements. Taking into account the presence of noise, (1b) and (1c) can be approximated by

$$\begin{aligned} \hat{\boldsymbol{\omega}} &\approx \tilde{\mathcal{R}}(\boldsymbol{\omega}_r - \hat{\mathbf{b}} + \mathbf{n}_w) - k_\omega(\mathbf{s}_\omega + \mathbf{n}_v) \\ \dot{\hat{\mathbf{b}}} &\approx -k_b(\mathbf{s}_\omega + \mathbf{n}_v) \end{aligned}$$

where $\mathbf{n}_w \in \mathbb{R}^3$ and $\mathbf{n}_v \in \mathbb{R}^3$ are zero-mean Gaussian random variables with second moments identical to those of ${}^B\hat{\mathbf{U}}{}^B\mathbf{U}^T(\boldsymbol{\omega}_r - \mathbf{b})$ and $[{}^B\mathbf{U}{}^B\hat{\mathbf{U}}^T - {}^B\hat{\mathbf{U}}{}^B\mathbf{U}^T]_\otimes$, respectively. These moments are computed in simulation environment using noisy measurements for the distances and angular rates. With this approximation, the error dynamics are described by

$$\begin{aligned} \dot{\tilde{\mathbf{q}}}_v &= -2k_\omega\tilde{q}_s^2\tilde{\mathbf{q}}_v \\ &\quad + \frac{1}{2}(\tilde{q}_s\mathbf{I} + [\tilde{\mathbf{q}}_v]_\times)(\tilde{\mathbf{b}} + \mathbf{n}_w - k_\omega\tilde{\mathcal{R}}^T\mathbf{n}_v) \\ \dot{\tilde{\mathbf{b}}} &= -4k_b\tilde{q}_s\tilde{\mathbf{q}}_v - k_b\mathbf{n}_v. \end{aligned}$$

Consider now the transformation $\boldsymbol{\xi}_1(t) = \mathbf{T}(t)\tilde{\mathbf{q}}_v(t)$, $\boldsymbol{\xi}_2(t) = \mathbf{T}(t)\tilde{\mathbf{b}}(t)$, where $\mathbf{T}(t)$ is given by (6). Linearizing the dynamics of the transformed system about the equilibrium point $(\tilde{\mathcal{R}}, \mathbf{b}) = (\mathbf{I}, \mathbf{0})$, we obtain the following linear system:

$$\dot{\boldsymbol{\xi}} = \bar{\mathbf{A}}\boldsymbol{\xi} + \bar{\mathbf{K}}\bar{\mathbf{C}}\boldsymbol{\xi} - \bar{\mathbf{K}}\mathbf{v} + \mathbf{w} \tag{18}$$

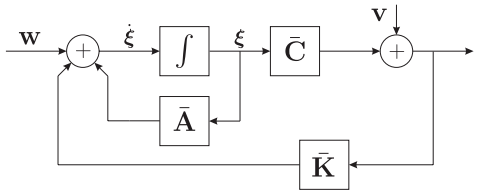

Fig. 2. Block diagram of the transformed system (18).

where

$$\bar{\mathbf{A}} = \begin{bmatrix} 0 & \frac{1}{2} \\ 0 & 0 \end{bmatrix} \quad \bar{\mathbf{K}} = \begin{bmatrix} k_\omega \mathbf{I} \\ 2k_b \mathbf{I} \end{bmatrix} \quad \bar{\mathbf{C}} = [2\mathbf{I}\ \mathbf{0}] \tag{19}$$

and

$$\mathbf{v} = \frac{\mathbf{T}}{2}\mathbf{n}_v \quad \mathbf{w} = \frac{\mathbf{T}}{2}\mathbf{n}_w.$$

It turns out that this system, whose block diagram is shown in Fig. 2, is in the Kalman–Bucy filter form (see [28] for more details) and therefore one can use the associated theory to compute suitable constant gains k_ω and k_b. This is accomplished by solving the following algebraic Riccati equation:

$$\mathbf{0} = \bar{\mathbf{A}}\bar{\mathbf{P}} + \bar{\mathbf{P}}\bar{\mathbf{A}}^T - \bar{\mathbf{P}}\bar{\mathbf{C}}^T\bar{\mathbf{R}}^{-1}\bar{\mathbf{C}}\bar{\mathbf{P}} + \bar{\mathbf{Q}}$$

where $\bar{\mathbf{R}}$ and $\bar{\mathbf{Q}}$ are covariance matrices of $\mathbf{v}$ and $\mathbf{w}$, respectively, and $\bar{\mathbf{P}}$ is the steady-state covariance matrix of the state $\boldsymbol{\xi}$. Notice that, since $\mathbf{T}$ is a rotation matrix, it does not affect the covariance of $\mathbf{v}$ and $\mathbf{w}$, hence $\bar{\mathbf{R}}$ and $\bar{\mathbf{Q}}$ can be obtained directly from the covariance of $\mathbf{n}_v/2$ and $\mathbf{n}_w/2$, respectively. The matrix of gains $\bar{\mathbf{K}}$ that minimizes $\bar{\mathbf{P}}$ is given by $\bar{\mathbf{K}} = \bar{\mathbf{P}}\bar{\mathbf{C}}\bar{\mathbf{R}}^{-1}$. Finally, the gains k_ω and k_b are obtained directly from (19).

V. Experimental Apparatus

A real-time prototype was developed comprising an inertial unit and a range measurement system, which was installed on a motion rate table that provided ground-truth data. In this section, we describe the experimental setup and the experiment carried out to validate the proposed technique.

A. Discrete-Time Implementation

An advantage of the continuous-time approach adopted in this brief is the large region of attraction of the desired equilibrium point. However, the nonlinear differential equations that constitute the observer are not in the form suitable for computer implementation, and hence it is necessary to obtain a discrete-time approximation of the original system. The key idea governing the selection of the numerical integration method is the fact that the rotation matrix belongs to the Lie group SO(3) and the intrinsic geometric properties of this group have to be preserved by the numerical integration algorithms. This is not guaranteed by the classical integration techniques such as Runge–Kutta methods, since these do not preserve polynomials invariants, like the determinant, with a degree greater than 3 [29, Theorem IV-3.3]. Therefore, we have implemented the proposed attitude observer resorting to the commutator-free Lie group method [30], which is a geometrical integration method and preserves the geometrical properties of the rotation group. This method leads to a singularity-free integration and does not require projection after the update because the integration already evolves on the underlying manifold.

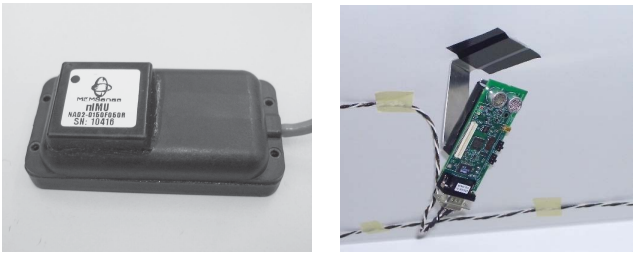

(a) (b)

Fig. 3. (a) Inertial unit Memsense nIMU. (b) Cricket mote.

B. Memsense nIMU

The angular rate measurements were acquired by a MemSense nIMU (Fig. 3) that contains a triad of rate gyros, a triad of accelerometers, and a triad of magnetometers. The data is received via an RS422 communication link. The rate gyros have a dynamic range of $\pm 150^\circ\ \mathrm{s}^{-1}$, and typical and maximum noise of 0.36 and $0.95^\circ\ \mathrm{s}^{-1}$ (1σ), respectively.

C. Cricket Localization System

The range measurements were obtained using the Cricket localization system [19], which is composed by a set of Cricket motes (Fig. 3). Each mote can be set as a beacon or as a receiver. In this experimental setup, we used four motes as beacons and four as receivers. This system relies on the fact that speed of sound in air (about $343\ \mathrm{m\,s}^{-1}$) is much lower than the speed of an RF signal (speed of light). Each beacon emits an ultrasonic pulse simultaneously with an RF signal containing the respective identification. When the RF signal is detected by a receiver, it uses the time difference of arrival with respect to the ultrasonic pulse to compute the propagation time and subsequently the distance between the emitter and the receiver. For this experiment, the Cricket motes firmware was slightly modified so that the beacons only emit a pulse when requested by an external source via the RS422 data link. With this configuration, the beacons can be commanded to emit sequentially, avoiding the collisions usually observed with this system. At each sampling cycle, all distances between the beacons and the receivers are computed, neglecting the time difference between each beacon transmission, which is a relatively good approximation given the proximity of the receivers with respect to the beacons. The range measurements have a resolution of 0.01 m. This system allows for a sampling frequency of 2 Hz.

D. Motion Rate Table

The system is installed on an Ideal Aerosmith Positioning and Rate Table Model 2103HT [23], see Fig. 4. This table provides precise triaxial angular position, rate, and acceleration measurements for development and testing of inertial

Fig. 4. Experimental setup.

components and systems. It has $\pm 0.0083^\circ$ position accuracy and $0.01\% \pm 0.0005^\circ\ \mathrm{s}^{-1}$ rate accuracy.

E. Observer Gains

The noise of the angular rate measurements is characterized by a biased Gaussian distribution with standard deviation given by 0.5443, 0.4756, and $0.5386^\circ\ \mathrm{s}^{-1}$ (1σ) for the x, y, and z axis, respectively. Regarding the range measurements, we consider a standard deviation of the measurements of 0.1 m. This value was slightly inflated to accommodate effects such as delays in the communications.

Based on the variance of the distance and angular rate measurements, the second moments of all channels of $\mathbf{n}_v$ and $\mathbf{n}_w$ are 0.2843 and $1.07\ 10^{-4}$, respectively. Consequently, as discussed in Section IV, the matrices $\bar{\mathbf{R}}$ and $\bar{\mathbf{Q}}$ are given by

$$\bar{\mathbf{R}} = \begin{bmatrix} 0.0702 & 0 & 0 \\ 0 & 0.0702 & 0 \\ 0 & 0 & 0.0702 \end{bmatrix}$$

$$\bar{\mathbf{Q}} = 10^{-4} \begin{bmatrix} 0.2614 & 0 & 0 \\ 0 & 0.2614 & 0 \\ 0 & 0 & 0.2614 \end{bmatrix}$$

and the Kalman gain matrix is given by

$$\bar{\mathbf{K}} = \begin{bmatrix} 0.0982 & 0 & 0 \\ 0 & 0.0982 & 0 \\ 0 & 0 & 0.0982 \\ 0.0193 & 0 & 0 \\ 0 & 0.0193 & 0 \\ 0 & 0 & 0.0193 \end{bmatrix}.$$

From this matrix, we extract the observer gains using the definition (19): $k_\omega = 0.0982$ and $k_b = 0.0096$.

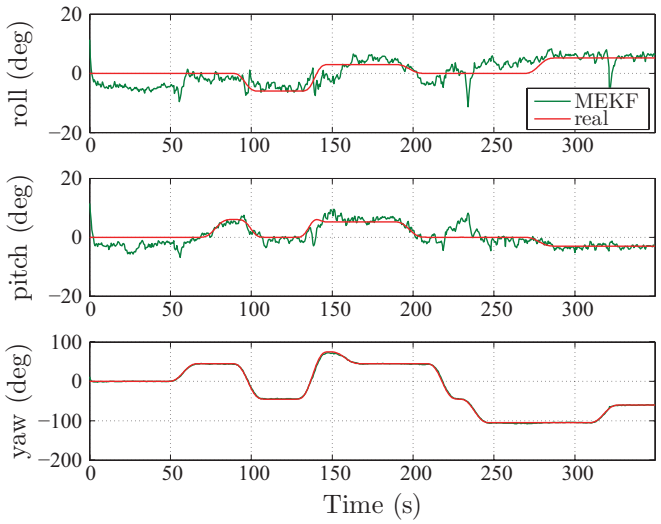

Fig. 5. Attitude estimates provided by the MEKF.

This set of gains is suitable in terms of local performance because, in the neighborhood of the origin, the nonlinear observer can be approximated by its linearization and the gains are designed so as to reduce the impact of the measurement noise on the estimation error.

VI. Experimental Results

This section presents experimental results that validate the applicability of the proposed solution, considering the reduced accuracy and low sampling frequency of the ultrasonic sensors. To guarantee that range measurements are available throughout the experiment, the performed trajectory is selected to ensure proper detection of ultrasonic pulses by the receiver transducers. Due to the high directionality of the Cricket ultrasound emitters [19], the trajectory is characterized by small angular displacements in roll and pitch. This restriction does not apply to the yaw angle, which can perform larger excursions. The results of the proposed nonlinear observer (NL observer) are compared with the common solution based on the MEKF [6] using the same initial conditions for both estimators.

Figs. 5 and 6 show the results provided by the MEKF and the time evolution of the attitude estimates obtained using the proposed solution, respectively. A large error on the initial estimates was purposely introduced to highlight the convergence rate of the estimates. The time evolution of the estimation errors for both the MEKF and the proposed attitude observer is shown in Fig. 7. From this figure, we conclude that both solutions successfully estimate the attitude, but the MEKF exhibits more sensitivity to outliers and large angular velocities. Finally, Fig. 8 depicts the time evolution of the rate gyro bias estimates of the MEKF and the nonlinear observer. This figure shows that the estimates converge to approximately constant values of bias. Some variations after the initial transient can be attributed to measurement errors, thermal fluctuations, and small changes in the real value of the rate gyro bias. Even in these conditions, the MEKF shows more oscillations on its estimates, which is undesirable.

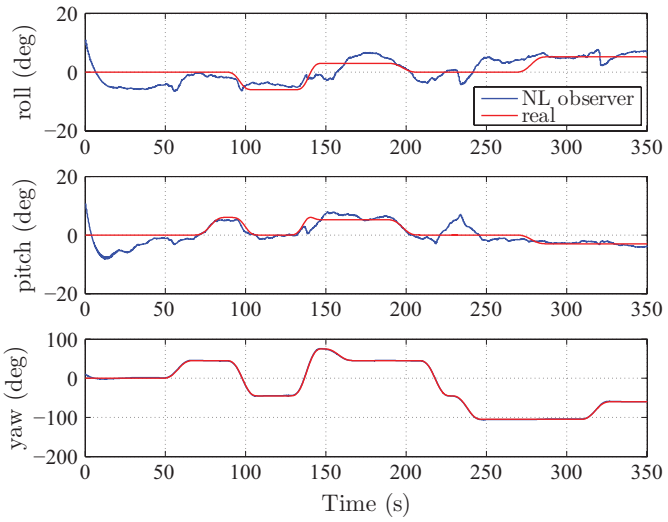

Fig. 6. Attitude estimates provided by the proposed solution.

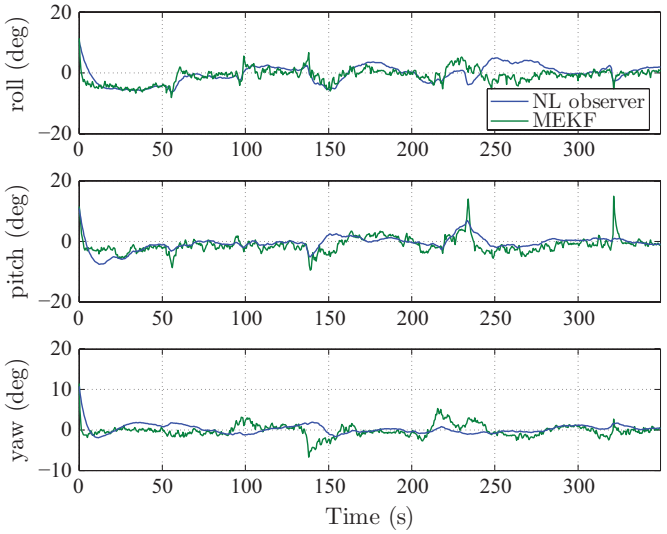

Fig. 7. Comparison of the estimation errors brought about by the use of the MEKF and the proposed attitude observer.

Bearing in mind the reduced accuracy of the ultrasonic range measurements, the standard deviations obtained with the observer after the initial transient are 2.4856° for roll, 1.5381° for pitch, and 0.6928° for yaw. By comparison, the standard deviations obtained with the MEKF are 1.7569°, 2.6918°, and 1.2412° for roll, pitch and yaw, respectively. From these results we can conclude that the proposed nonlinear observer has better accuracy than the MEKF in two of the Euler angles. In spite of this, the main advantage of the nonlinear observer when compared with the MEKF is the very large region of attraction. For our dataset, with a considerable tuning effort, it was possible to tune the MEKF so that the stability is verified even for large initial errors. However, different operating conditions may compromise stability, which might not be acceptable for critical scenarios. In contrast, the nonlinear observer is easily tuned and allows straightforward implementation.

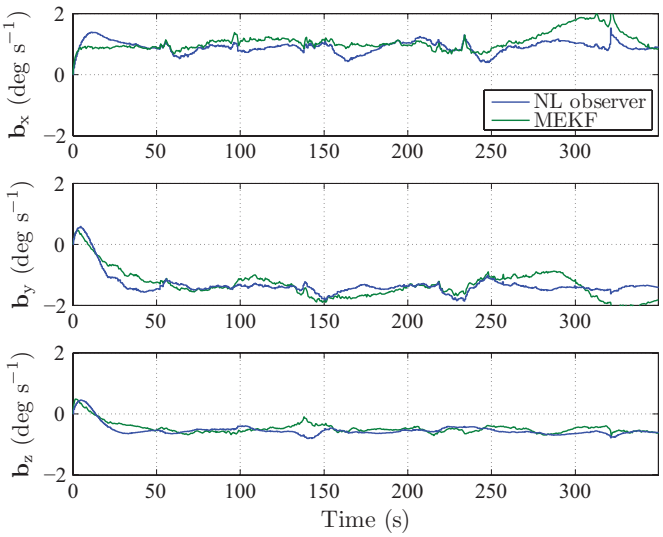

Fig. 8. Angular rate bias estimates from the MEKF and from the proposed nonlinear observer.

VII. Conclusion

In this brief, a nonlinear attitude observer defined on the SO(3) manifold that relies on inertial and range measurements was presented. The presence of static bias in angular velocity measurements was considered and its value estimated by the observer. Exponential convergence of the estimates to the desired equilibrium points was established. An experimental prototype validated the good performance of the proposed solution when resorting to a three-axis motion rate table. Future work will be devoted to the implementation of the system on board an unmanned aerial vehicle.

Acknowledgment

The authors would like to acknowledge the contribution of P. Batista in the calibration of the positions of the Cricket motes.

References

[1] G. Wahba, "Problem 65-1: A least squares estimate of satellite attitude," *SIAM Rev.*, vol. 7, no. 3, p. 409, Jul. 1965.
[2] B. Anderson and J. Moore, *Optimal Filtering*. New York: Dover, 1979.
[3] E. Lefferts, F. Markley, and M. Shuster, "Kalman filtering for spacecraft attitude estimation," *J. Guidance Control Dynam.*, vol. 5, no. 5, pp. 417–429, 1982.
[4] Y. Yang and J. Farrell, "Two antennas GPS-aided INS for attitude determination," *IEEE Trans. Control Syst. Technol.*, vol. 11, no. 6, pp. 905–918, Nov. 2003.
[5] J. Crassidis, "Sigma-point Kalman filtering for integrated GPS and inertial navigation," *IEEE Trans. Aerosp. Electron. Syst.*, vol. 42, no. 2, pp. 750–756, Apr. 2006.
[6] F. Markley, "Attitude error representations for Kalman filtering," *J. Guidance Control Dynam.*, vol. 26, no. 2, pp. 311–317, 2003.
[7] S. Bonnabel, P. Martin, and E. Salaun, "Invariant extended Kalman filter: Theory and application to a velocity-aided attitude estimation problem," in *Proc. 48th IEEE Decision Control Conf.*, Shanghai, China, Dec. 2009, pp. 1297–1304.
[8] J. Thienel and R. Sanner, "A coupled nonlinear spacecraft attitude controller and observer with an unknown constant gyro bias and gyro noise," *IEEE Trans. Autom. Control*, vol. 48, no. 11, pp. 2011–2015, Nov. 2003.
[9] J. Pflimlin, T. Hamel, and P. Souères, "Nonlinear attitude and gyroscope's bias estimation for a VTOL UAV," *Int. J. Syst. Sci.*, vol. 38, no. 3, pp. 197–210, Mar. 2007.

[10] S. Bonnabel, P. Martin, and P. Rouchon, "Symmetry-preserving observers," *IEEE Trans. Autom. Control*, vol. 53, no. 11, pp. 2514–2526, Dec. 2008.

[11] J. Kinsey and L. Whitcomb, "Adaptive identification on the group of rigid-body rotations and its application to underwater vehicle navigation," *IEEE Trans. Robot.*, vol. 23, no. 1, pp. 124–136, Feb. 2007.

[12] R. Mahony, T. Hamel, and J.-M. Pflimlin, "Nonlinear complementary filters on the special orthogonal group," *IEEE Trans. Autom. Control*, vol. 53, no. 5, pp. 1203–1218, Jun. 2008.

[13] P. Martin and E. Salaün, "Design and implementation of a low-cost observer-based attitude and heading reference system," *Control Eng. Pract.*, vol. 18, no. 7, pp. 712–722, 2010.

[14] H. F. Grip, T. I. Fossen, T. A. Johansen, and A. Saberi, "Attitude estimation using biased gyro and vector measurements with time-varying reference vectors," *IEEE Trans. Autom. Control*, vol. 57, no. 5, pp. 1332–1338, May 2012.

[15] N. Chaturvedi and N. McClamroch, "Almost global attitude stabilization of an orbiting satellite including gravity gradient and control saturation effects," in *Proc. Amer. Control Conf.*, Minneapolis, MN, Jun. 2006, pp. 1–6.

[16] D. Fragopoulos and M. Innocenti, "Stability considerations in quaternion attitude control using discontinuous Lyapunov functions," in *Proc. IEEE Control Theory Appl.*, vol. 151. May 2004, no. 3, pp. 253–258.

[17] M. Malisoff, M. Krichman, and E. Sontag, "Global stabilization for systems evolving on manifolds," *J. Dynam. Control Syst.*, vol. 12, no. 2, pp. 161–184, Apr. 2006.

[18] H. Nijmeijer and T. Fossen, *New Directions in Nonlinear Observer Design*. New York: Springer-Verlag, 1999.

[19] N. Priyantha, A. Chakraborty, and H. Balakrishnan, "The Cricket location-support system," in *Proc. 6th Annu. ACM Int. Conf. Mobile Comput. Netw.*, Aug. 2000, pp. 32–43.

[20] J. Vasconcelos, C. Silvestre, and P. Oliveira, "A nonlinear observer for rigid body attitude estimation using vector observations," in *Proc. 17th IFAC World Congr.*, Seoul, Korea, Jul. 2008, pp. 8599–8604.

[21] S. Brás, J. Vasconcelos, C. Silvestre, and P. Oliveira, "Pose observers for unmanned air vehicles," in *Proc. Eur. Control Conf.*, Budapest, Hungary, Aug. 2009, pp. 3989–3994.

[22] S. Brás, C. Silvestre, P. Oliveira, J. Vasconcelos, and R. Cunha, "An experimentally validated attitude observer based on range and inertial measurements," in *Proc. 18th IFAC World Congr.*, Milan, Italy, Sep. 2011, pp. 1–6.

[23] Ideal Aerosmith Inc. (2006). *2103HT Multiaxis Table Data Sheet, Rev C 687*, Grand Forks, ND [Online]. Available: http://www.ideal-aerosmith.com/

[24] J. Smith and J. Abel, "The spherical interpolation method of source localization," *IEEE J. Oceanic Eng.*, vol. 12, no. 1, pp. 246–252, Jan. 1987.

[25] R. Murray, Z. Li, and S. Sastry, *A Mathematical Introduction to Robotic Manipulation*. Boca Raton, FL: CRC, 1994.

[26] W. Rugh, *Linear System Theory*, 2nd ed. Englewood Cliffs, NJ: Prentice-Hall, 1996.

[27] H. Khalil, *Nonlinear Systems*, 3rd ed. Englewood Cliffs, NJ: Prentice-Hall, 2002.

[28] R. Kalman and R. Bucy, "New results in linear filtering and prediction theory," *Trans. ASME, J. Basic Eng.*, vol. 83, pp. 95–108, Mar. 1961.

[29] E. Hairer, C. Lubich, and G. Wanner, *Geometric Numerical Integration: Structure-Preserving Algorithms for Ordinary Differential Equations*. New York: Springer-Verlag, 2002.

[30] E. Celledoni, A. Marthinsen, and B. Owren, "Commutator-free Lie group methods," *Future Generat. Comput. Syst.*, vol. 19, no. 3, pp. 341–352, Apr. 2003.